College of Chinese Medicine[1], Beijing University of Chinese Medicine, Beijing; College of Pharmaceutical Science[2], Zhejiang University, Hangzhou; Jiangsu Kanion Pharmaceutical CO., LTD[3], Lianyungang, China

Acousto-optic tunable filter near-infrared spectroscopy for in-line monitoring liquid-liquid extraction of *Gardenia jasminoides* Ellis based on statistical analysis

Sha Wu[1], Ye Jin[2], Qi-An Liu[3], Jian-Xiong Wu[3], Yu-An Bi[3], Zhen-Zhong Wang[3], Wei Xiao[3]

Received November 02, 2014, accepted December 13, 2014

Prof. Wei Xiao, Jiangsu Kanion Pharmaceutical CO., LTD, 58 Haichang Road, Lianyungang 222000, China
xw_kanion@163.com

Pharmazie 70: 640–645 (2015) *doi: 10.1691/ph.2015.4173*

This study aimed to monitor liquid-liquid extraction of *Gardenia jasminoides* Ellis (Zhizi in Chinese) using in-line near-infrared spectroscopy. Shanzhiside (SZS), deacetyl asperulosidic acid methyl ester (DAAME), genipin-1-β-D-gentiobioside (GG), geniposide (GS), total acids (TA) and soluble solid content (SSC) were selected as quality control indicators, and measured by reference methods. Both partial least-squares regression (PLSR) and back propagation artificial neural networks (BP-ANN) were applied to create models to predict the content of above indicators. Paired-samples t-test and nonparametric test were used to compare differences in predictive values between two models of each indicator. Relative standard error of prediction (RSEP) and mean absolute percentage error (MAPE) were used to evaluate the predictive accuracy of the established models. The results showed that there was no significant difference in predicting DAAME, GS and TA between two models. However, PLSR model gave better accuracy in predicting GG and SZS than BP-ANN model. The BP-ANN model of SSC was better than PLSR model. This study shows that NIR spectroscopy can be used for rapid and accurate analysis of quality control indicators in the liquid-liquid extraction of Zhizi. Simultaneously, this study can serve as technical support for the application of NIR spectroscopy in the industrial production process.

1. Introduction

Gardenia jasminoides Ellis (Zhizi in Chinese) is one of the fundamental herbs in Reduning injection, which has traditionally been used for the treatment of upper respiratory tract infections in China. The main active compounds in Zhizi are iridoid glycosides, caffeoylquinic acids and crocins (Liu et al. 2013), such as shanzhiside (SZS), deacetyl asperulosidic acid methyl ester (DAAME), genipin-1-β-D-gentiobioside (GG), geniposide (GS) and chlorogenic acid (CA).

Liquid-liquid extraction separates one or several substances present in a liquid phase by the addition of another liquid phase in which these substances are transferred preferentially (Khooshechin et al. 2013). Nevertheless, the extraction efficiency can be affected by a lot of process parameters, such as temperature, initial density of starting material, volume of solvent, flow rate of solvent and pH of solution (Cui et al. 2012). These factors can have a large impact on the downstream unit operations such as filtration and drying, as well as on the final drug quality. Consequently, process analytical technology (PAT) is necessary to be applied for real-time quality control in liquid-liquid extraction process.

Near-infrared (NIR) spectroscopy is one of the most efficient tools in the pharmaceutical industry due to its high resolution, fast scanning speed, good stability and non-destructive nature towards samples (Reich 2005). The combination of high dimension optical fibers and fiber optic probes allows remote in-line measurements in the production workshop (Schaefer et al. 2013). Many researches have demonstrated that NIR spectroscopy is a robust method for quantitative analysis of the content of active pharmaceutical ingredients (API) (Li et al. 2013; Schönbichler et al. 2013; Dong et al. 2010) and real-time monitoring of complex pharmaceutical production processes (Jin et al. 2013; Liu et al. 2013; Wu et al. 2011).

This study aimed to monitor liquid-liquid extraction of Zhizi using in-line NIR spectroscopy. SZS, DAAME, GG and GS are the principal bioactive components in Zhizi. Total acid (TA) is the total content of the caffeoylquinic acids on behalf of CA. The soluble solid content (SSC) is the percentage of the total content of substances dissolved in the extraction solution and indicates the purification ability of liquid-liquid extraction. Therefore, SZS, DAAME, GG, GS, TA and SSC were selected as quality control indicators. Models predicting each indicator were built based on partial least-squares regression (PLSR) and back propagation artificial neural networks (BP-ANN) and were evaluated on the predictive accuracy by a prediction set.

2. Investigations and results

2.1. Results of reference assays

The UPLC chromatogram of extraction solution is depicted in Fig. 1, indicating that a baseline separation of the measured peaks could be achieved. The parameters of retention time (t_R), linear range, calibration curve, coefficients of determina-

Table 1: Methodology parameters and calibration curves of UPLC method

Compounds	t_R (min)	Linear range (μg/mL)	Calibration curve	R^2	Repeatability (RSD %)	Stability (24 h, RSD %)	Recovery (%)
SZS	4.27	6.08-60.84	y = 5.829x - 0.775	0.9999	1.07	1.18	99.97
DAAME	5.36	14.95-149.52	y = 6.481x– 1.699	0.9999	0.73	1.11	97.09
GG	11.48	14.05-140.46	y = 3.355x + 1.281	0.9999	1.05	1.21	97.55
GS	13.52	177.90-1779.00	y = 6.787x + 30.59	1	0.69	1.05	99.27

Table 2: Methodology parameters and calibration curve of UV spectroscopy method

Compound	Linear range (μg/mL)	Calibration curve	R^2	Repeatability (RSD %)	Stability (90 min, RSD %)	Recovery (%)
TA	5.12−25.62	y = 53.922x + 0.00235	0.9999	0.55	0.67	100.50

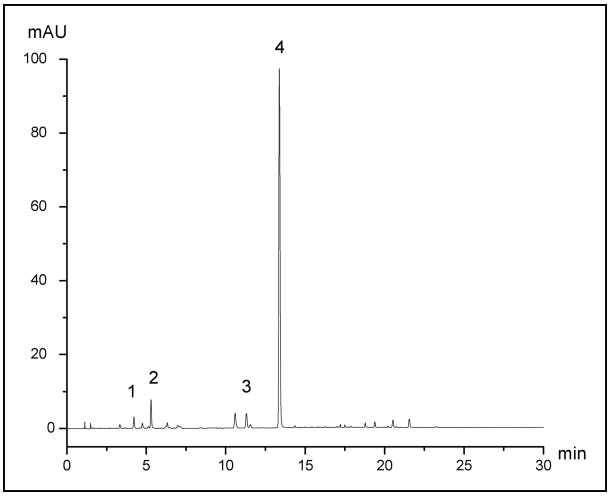

Fig. 1: UPLC chromatogram of extraction solution (1, SZS; 2, DAAME; 3, GG; 4, GS).

tion (R^2), repeatability, stability and recovery of UPLC method (Table 1) and UV spectroscopy method (Table 2) were verified. Variations in the content of the indicators are of crucial importance for modeling. Therefore, the content was statistically analyzed by descriptive indexes, which included mean, range and standard deviation (SD), as listed in Table 3. The content ranges in the calibration set covered the ranges in the prediction set, implying a favorable variability for multivariate calibration models.

2.2. Dynamic curves during the liquid-liquid extraction process

The dynamic curves for SZS, DAAME, GG, GS, SSC and TA in batch 131203 are shown in Fig. 2. SZS, DAAME and GG had a slight decline. GS dropped from 37 mg/mL to 7.3 mg/mL. TA decreased from 8.6 mg/mL to 1.6 mg/mL. SSC dropped sharply from 78 mg/mL to 18 mg/mL with the continuous dissolution of substances.

2.3. Selecting spectral wavelength

The peak assignment to specific chemical groups with accuracy is difficult, but the bands of interest could be identified. Spectra are characterized by two principle water absorption bands of around 1450 nm and 1920-1950 nm (Namkung et al. 2008). The first band, with weak absorbance, is observed at 1200 nm and can be considered as the second overtone of the CH stretching vibrations of CH_3, CH_2, and CH = CH (Bellincontro et al. 2012). The third band, centered around 1570 nm, can be attributed to the first overtone of the OH bond (Li et al. 2014). The two bands located at 1720 nm and 1750 nm correspond to the first overtone of the CH stretching vibrations of CH_3, CH_2, and CH = CH (Kuligowski et al. 2012). By analyzing the effect of different wavelength ranges on model performance, 1100-1900 nm was finally selected for SZG, DAAME, GG, GS and SSC, and 1390 nm-2080 nm was chosen for TA.

2.4. Preprocessing spectral data

Spectral preprocessing tools can significantly eliminate random noise interference and remove the baseline drift (Teye et al. 2013). To correct the baseline drift caused by background color of samples, derivative pretreatment including first derivative and second derivative was usually adopted for developing calibration models (Wu et al. 2013). In the derivation process, high frequency noise signals may be magnified, therefore the spectrum should be smoothed to filter noise (Chalus et al. 2007). To eliminate the scatter effects, multiplicative signal correction (MSC) and standard normal variate (SNV) were used. As shown in Table 4, different preprocessing methods can lead to different

Table 3: Descriptive statistics of the reference content in the extraction solution

	Calibration set			Prediction set		
	Mean (mg/mL)	Range (mg/mL)	S.D. (mg/mL)	Mean (mg/mL)	Range (mg/mL)	S.D. (mg/mL)
GS	16.48	4.74−36.10	8.17	12.97	5.17−31.24	8.13
DAAME	1.20	0.57−2.12	0.38	1.00	0.66−1.66	0.27
GG	1.51	0.91−2.36	0.36	1.28	0.93−2.01	0.25
SSC	46.03	15.41−93.33	21.27	33.10	18.82−87.75	17.65
SZS	0.52	0.30−0.83	0.13	0.43	0.31−0.74	0.09
TA	4.97	1.57−9.69	2.27	4.01	1.85−8.44	1.97

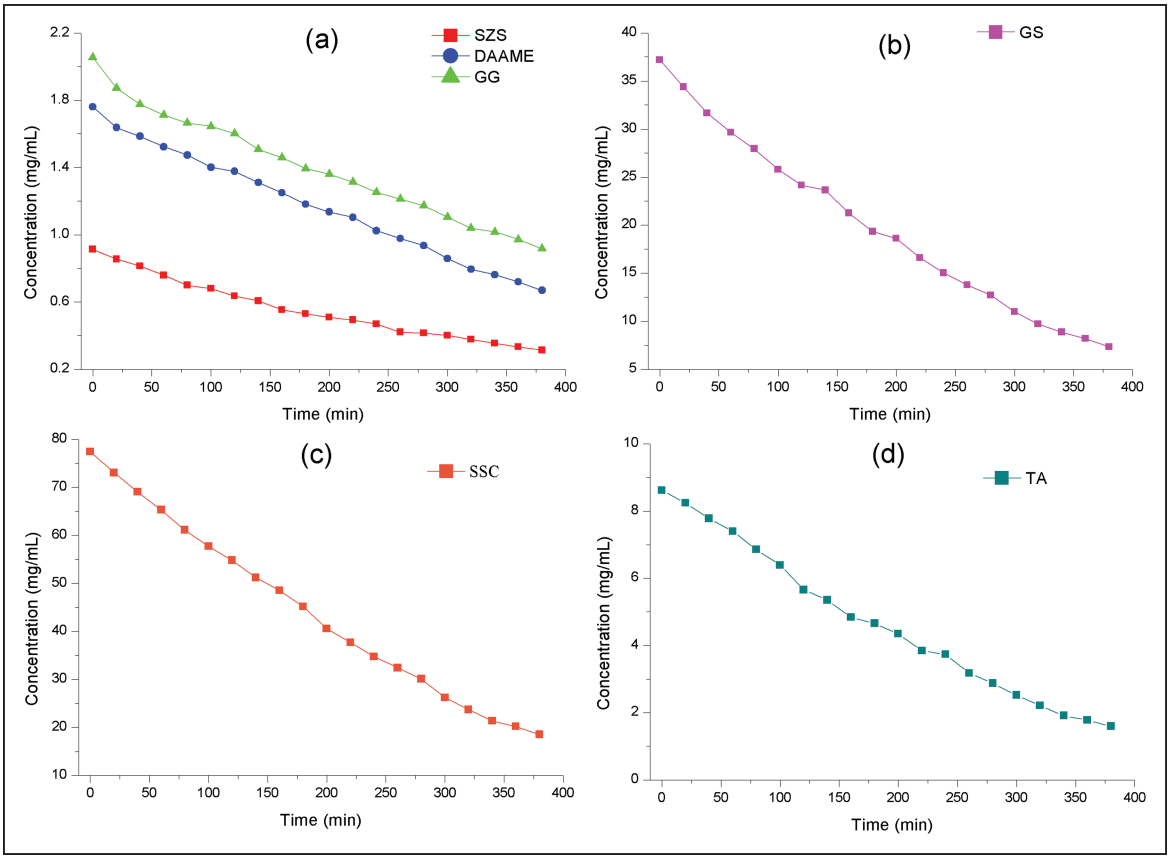

Fig. 2: Time evolution of SZS (a), DAAME (a), GG (a), GS (b), SSC (c) and TA (d) in batch 131203 during the liquid-liquid extraction of Zhizi.

models, and the best model was found to be the one built on data pretreated using first derivative, MSC and Savitzky-Golay smoothing (a 7-point smoothing and a third-order polynomial). The raw spectra and the spectra obtained with first derivative, MSC and Savitzky-Golay smoothing are shown in Fig. 3.

2.5. Establishing the PLSR model

Before building calibration models, spectral datasets were analyzed through principal component analysis (PCA). The spectral data matrix X is decomposed into a few new variables, called principal components (PCs), with aim to maximize the explained

Table 4: Influence of different spectral pretreatments on performance of PLS models

Compound	Pretreatments	Calibration set		Validation set	
		R	RMSEC(mg/mL)	R	RMSECV(mg/mL)
GS	raw spectra	0.9905	1.6773	0.9886	1.9531
	1st derivative, MSC and Savitzky-Golay smoothing	0.9935	1.2317	0.9925	1.3223
	2nd derivative, SNV and Savitzky-Golay smoothing	0.9894	1.8727	0.9854	2.1064
DAAME	raw spectra	0.9828	0.1029	0.9751	0.1230
	1st derivative, MSC and Savitzky-Golay smoothing	0.9918	0.0608	0.9882	0.0728
	2nd derivative, SNV and Savitzky-Golay smoothing	0.9874	0.0879	0.9841	0.1075
GG	raw spectra	0.9747	0.1223	0.9695	0.1425
	1st derivative, MSC and Savitzky-Golay smoothing	0.9923	0.0569	0.9900	0.0647
	2nd derivative, SNV and Savitzky-Golay smoothing	0.9885	0.0820	0.9767	0.1182
SSC	raw spectra	0.9833	3.6136	0.9817	3.9271
	1st derivative, MSC and Savitzky-Golay smoothing	0.9939	3.0854	0.9930	3.2959
	2nd derivative, SNV and Savitzky-Golay smoothing	0.9938	3.0981	0.9910	3.4445
SZS	raw spectra	0.9640	0.0415	0.9579	0.0441
	1st derivative, MSC and Savitzky-Golay smoothing	0.9754	0.0398	0.9723	0.0422
	2nd derivative, SNV and Savitzky-Golay smoothing	0.9782	0.0402	0.9693	0.0474
TA	raw spectra	0.9773	0.3121	0.9725	0.3578
	1st derivative, MSC and Savitzky-Golay smoothing	0.9868	0.2461	0.9959	0.2766
	2nd derivative, SNV and Savitzky-Golay smoothing	0.9739	0.3341	0.9651	0.3923

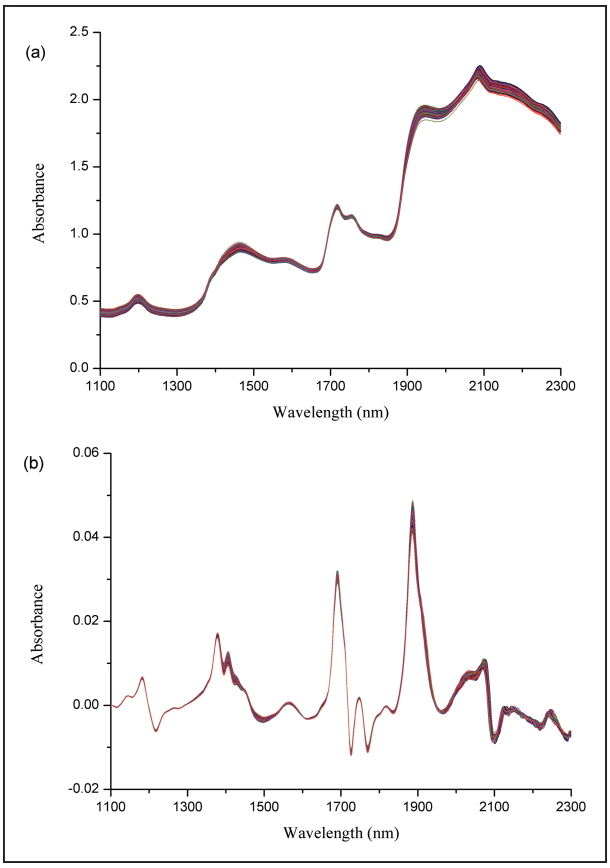

Fig. 3: Raw spectra (a) and the spectra with first derivative, MSC and Savitzky-Golay smoothing pretreatment (b).

variance in the matrix X (Carey et al. 1975; Luna et al. 2013). Taking GS as example, X variance was explained by PC1 72% and PC2 16% and Y variance was explained by PC1 41% and PC2 24%. Five PCs were selected for the explanation of total X variance 100% and Y variance 98%.

Outliers were detected based on the leverage level and the residual of Y variance (Wu et al. 2012). Taking GS as representative, observation 81 and 93 had a large residual and a relative small leverage level, indicating they were outlying observations and should be removed from the GS calibration model.

After PCA, detecting outliers and a full cross-validation, the PLSR model of each indicator was constructed. As seen in Table 5, the established models had good performance both in calibration and cross-validation sets. The correlation coefficient (R) was high, and the root mean square errors of calibration (RMSEC) was approximate to the root mean square errors of cross-validation (RMSECV).

2.6. Establishing the BP-ANN model

BP-ANN was applied to build the nonlinear relationship between spectral signals and reference data. BP-ANN algorithms were carried out by the ANN lab toolbox in Matlab R2012a software (MathWorks Inc., USA). BP-ANN network was composed of three layers. The network was constructed with trainlm training function, learngdm learning function and tansig transferred function. The least learning rate was set as 0.6. The network was trained by the gradient descend method and the minimum gradient was set as 1.0×10^{-5}. The biggest epochs were set as 1,000. Taking GS as example, different numbers of nodes in the hidden layer were compared. When the nodes were 10, the RMSEC and RMSECV were lower than 1.0 mg/mL, which satisfied our precision requirements (Table 6). Therefore, ten nodes were chosen in the network. As can be observed in Table 5, BP network, with higher R and lower RMSEC and RMSECV, showed superior generalization in quantitative analysis of GS, DAAME, GG, SSC, SZS and TA than the corresponding PLSR model. This can be accounted for nonlinear relationship is taken into consideration in BP network (Roggo et al. 2007), while PLSR method only has the ability to quantify information in linear ways.

2.7. In-line quantitative monitoring

The PLSR and BP-ANN models for GS, DAAME, GG, SSC, SZS and TA were validated with 20 samples in a prediction set. Statistical parameters such as R, root mean square errors of prediction (RMSEP) and relative standard error of prediction (RSEP) were used to assess the predictive performance (Table 5). It was noticed that all the RSEP values were lower than 8%, which satisfied the prediction precision in NIR analysis (Jin et al. 2013). In order to evaluate the predictive percentage errors, mean absolute percentage error (MAPE) was introduced as a new indicators (Table 5). The MAPE value of each compound was much higher than the RSEP value. Especially, the MAPE values of both models for SZS were higher than 20%. This was probably caused by the low content of SZS in the extraction solution. GG and TA obviously presented satisfactory fitting results and small prediction errors with RSEP < 2% and MAPE < 10%. Overall, PLSR models displayed better predictive performance than BP-ANN models with low RSEP and MAPE except for SSC. Maybe this because over-fitting issues easily decease the predictive performance of the ANN models (Ni et al. 2014). As for SSC, as the sum of substances dissolved in the extraction solution, it contains a variety of complicated chemical ingredients (Zhu et al. 2008). Therefore, the relationship between spectra and SSC is more inclined to be non-linear rather than linear.

Statistical analysis was used to compare differences in predictive values between PLSR and BP-ANN. The normality test rejects the hypothesis of normality when the p-value is less than 0.05. A t-test for paired samples is applied for normal data, while a Wilcoxon rank sum test is used for non-normal data. The results showed that there was no significant difference in predicting DAAME, GS and TA between PLSR and BP-ANN, but a significant difference in predicting GG, SZS and SSC. The PLSR models of GG and SZS had lower RSEP values and MAPE values than their BP-ANN models. This indicated that the PLSR method was more suitable for GG and SZS. As for SSC, the BP-ANN model with lower RSEP value and MAPE value was slightly better than the PLSR model.

3. Discussion

This study developed a NIR spectroscopy method to monitor the content of quality control indicators in liquid-liquid extraction of Zhizi. There was little bubble interference in the spectral acquisition, which may be due to the stable flow rate of extraction solvent. However, the fiber optic probes were easy to block and cause a decline in absorbance value. It is recommended to install a Y-type strainer or a belt filter to intercept solid particles. A high-pressure water gun is also available for fully automatic cleaning the filters.

As reported, black-box models usually perform better than linear models (Shi et al. 2013; Nie et al. 2013; Zhang et al. 2008; Zhu et al. 2007; Chen et al. 2012). However, statistical tests are rarely used to weigh the predictive accuracy. In this research, paired-samples t-test and nonparametric tests were used to compare the differences between PLSR models and BP-ANN models. The

Table 5: Statistics of the optimal models for liquid-liquid extraction of Zhizi using PLSR and BP-ANN methods

		Calibration set		Validation set			Prediction set		
		R	RMSEC(mg/mL)	R	RMSECV(mg/mL)	R	RMSEP(mg/mL)	RSEP%	MAPE%
GS	PLSR	0.9935	1.2317	0.9925	1.3223	0.9835	1.6569	2.86	9.17
	BP-ANN	0.9940	0.8511	0.9931	0.9417	0.9893	1.7611	3.04	12.71
DAAME	PLSR	0.9918	0.0608	0.9882	0.0728	0.9495	0.1404	3.15	13.06
	BP-ANN	0.9920	0.0489	0.9902	0.0504	0.9668	0.1499	3.37	15.32
GG	PLSR	0.9923	0.0569	0.9900	0.0647	0.9571	0.0971	1.70	6.75
	BP-ANN	0.9938	0.0400	0.9913	0.0465	0.9769	0.1074	1.88	7.92
SSC	PLSR	0.9939	3.0854	0.9930	3.2959	0.9756	3.7819	2.55	12.18
	BP-ANN	0.9948	2.1743	0.9941	2.3328	0.9922	3.5613	2.41	10.69
SZS	PLSR	0.9754	0.0398	0.9723	0.0422	0.9768	0.0996	4.81	22.12
	BP-ANN	0.9816	0.0233	0.9744	0.0373	0.9757	0.1298	6.27	29.71
TA	PLSR	0.9868	0.2461	0.9959	0.2766	0.9915	0.3214	1.79	8.23
	BP-ANN	0.9984	0.1339	0.9962	0.1679	0.9855	0.3378	1.88	8.70

Table 6: Influence of different nodes in the hidden layer on performance of GS BP-ANN model

Number of nodes	Calibration set		Validation set	
	R	RMSEC (mg/mL)	R	RMSECV (mg/mL)
1	0.9282	2.8569	0.9067	3.4418
2	0.9428	2.3012	0.9355	3.0835
3	0.9593	1.9019	0.9415	2.6714
4	0.9617	1.7756	0.9543	2.3816
5	0.9701	1.5073	0.9678	2.0102
6	0.9763	1.3558	0.9715	1.8325
7	0.9838	1.2530	0.9779	1.6921
8	0.9907	1.1320	0.9856	1.4776
9	0.9911	1.0717	0.9890	1.2511
10	0.9940	0.8511	0.9931	0.9417
11	0.9945	0.8057	0.9933	0.9213
12	0.9937	0.7356	0.9895	0.8585

results indicated that both methods were suitable for DAAME, GS and TA, except GG and SZS tending to PLSR and SSC tending to BP-ANN.

Considering the content of indicators varied largely during the liquid-liquid extraction process (Fig. 2), it was necessary to rapidly monitor the concentration of important indicators. This paper demonstrated that NIR spectroscopy could be well applied in the liquid-liquid extraction of traditional Chinese medicine production process, creating a reliable process measurement and ensuring stable product quality.

4. Experimental

4.1. Materials

Reference substances of CA, DAAME and GS were purchased from National Institutes for Food and Drug Control (Beijing, China). GG was purchased from Chengdu Preferred Biotechnology Co., LTD. SZS was purchased from BioBioPha Co., LTD. HPLC grade acetonitrile was obtained from Tedia Company (Fairfield, USA). Deionized water was obtained from a Mill-Q water purifier system (Millipore, Bedford, MA, USA). All the other reagents utilized in the article were of analytical grade.

4.2. Liquid-liquid extraction process

The countercurrent extraction column is packed with stainless-steel Raschig rings (Xiong et al. 2012). A pipe from its liquid outlet valve extends to the storage tank. Firstly, solution pumped into the column from the top. Next, the water-saturated 1-butanol used as extraction solvent was continuously pumped into the column from the bottom. The extraction solution began to flow out of the column after adding 1-butanol for two hours. A valve sample cell was installed into the pipeline to collect extraction solution.

4.3. Spectral collection

A Luminar 3060 acousto-optic tunable filter near-infrared (AOTF-NIR) spectrometer (Brimrose Co., USA) was used with SNAP 3.0 software for acquiring spectra and Unscrambler 7.8 software (Camo Software AS, Norway) for processing data. Two immersion transmission probes, optical path length of 2 mm, were immersed into the solution to collect spectra at 20 s intervals automatically. The probes were connected to the spectrometer by an optical fiber. The spectral range was from 1,100 nm to 2,300 nm with a wavelength increment of 2 nm.

4.4. Sample collection

During the liquid-liquid extraction process, samples were collected with a volume of 80 mL every 20 min at the same time the sampling time was recoded. According to the sampling time, the corresponding spectrum was selected from the continuous spectra. Eleven batches of samples were obtained, ten for model development and one for assessing the predictive accuracy of the established model. Each sample was marked as batch number -sampling order, e. g., 131203-1, meaning the first sample of batch 131203.

4.5. Reference assays

A ultra-high performance liquid chromatography (UPLC) method was developed for measuring the content of SZS, DAAME, GG and GS. The chromatographic analysis was performed on an Agilent 1290 series apparatus (Agilent Technologies, USA), equipped with a quaternary bump, an online vacuum degasser, an auto-sampler, a thermostatic column compartment and a diode-array detector. All the modules were controlled by the Agilent ChemStation software. The chromatographic separation was undertaken on an Agilent ZORBAX SB-C18 column (100 mm × 3.0 mm, 1.8 μm) at 30 °C. Solvent A [acetonitrile] and solvent B [aqueous phosphoric acid solution (0.1%, v/v)] were used as mobile phase for gradient elution (0-10 min: 5-10% A; 10-15 min: 10-20% A; 15-30 min: 20-30% A). The detection wavelength was set at 238 nm. The flow rate was 0.4 mL/min and

the injection volume was 2 μL. The solution was centrifuged at 10,000 rpm for 10 min and then diluted to 20 mL with methanol-water (50:50, v/v). The supernatant fluid was passed through a 0.22 μm syringe filter, and 2 μL of filtrate was injected into the UPLC system for analysis.

A ultraviolet (UV) spectroscopy method was used to analyze the content of TA. Different volume of CA standard solution was precisely transferred to a 20 mL flask, respectively, and added methanol-water (50:50, v/v) to scale as reference solution. The reference solution was scanned by a Shimadzu UV/VIS spectrometer 2700 (Shimadzu, JAPAN) with methanol-water (50:50, v/v) as blank solution. The absorbance value A1 was measured at 324 nm and A2 was measured at 400 nm. The calibration curve was constructed by plotting the concentration (x, mg/mL) versus the absorbance value (y, y = A1-A2).

The SSC was determined by drying 5 mL centrifuged solution at 105 °C to a constant weight. The results are expressed in wt. mg/mL.

Acknowledgements: We gratefully acknowledge financial support provided by the National Science and Technology Major Project of the Ministry of Science and Technology of China "Key New Drug Creation and Manufacturing Program"(Grant nos.2013ZX09402203).

References

Bellincontro A, Taticchi A, Servili M, Esposto S, Farinelli D, Mencarelli F (2012) Feasible application of a portable NIR-AOTF tool for on-field prediction of phenolic compounds during the ripening of olives for oil production. J Agricult Food Chem 60: 2665–2673.

Carey RN, Wold S, Westgard JO (1975) Principal component analysis: an alternative to "referee" methods in method comparison studies. Anal Chem 47: 1824–9.

Chalus P, Walter S, Ulmschneider M (2007) Combined wavelet transform–artificial neural network use in tablet active content determination by near-infrared spectroscopy. Anal Chim Acta 591: 219–224.

Chen Q, Ding J, Cai J, Zhao J (2012) Rapid measurement of total acid content (TAC) in vinegar using near infrared spectroscopy based on efficient variables selection algorithm and nonlinear regression tools. Food Chem 135: 590–595.

Cui Z, Cai M, Song C, Hilaire N, Wang Y (2012) Effects of different pretreatments on dynamic countercurrent extraction of polysaccharides from Ganoderma. Sep Purif Technol 85: 61–68.

Dong Q, Zang H, Liu A, Yang G, Sun C, Sui L, Wang P, Li L (2010) Determination of molecular weight of hyaluronic acid by near-infrared spectroscopy. J Pharm Biom Anal 53: 274–278.

Jin Y, Ding H, Liu X, Wan X, Luan L, Wu Y (2013) Investigation of an on-line detection method combining near infrared spectroscopy with local partial least squares regression for the elution process of sodium aescinate. Spectrochimica Acta Part A: Mol Biomol Spectrosc 109: 68–78.

Jin Y, Wu Z, Liu X, Wu Y (2013) Near infrared spectroscopy in combination with chemometrics as a process analytical technology (PAT) tool for on-line quantitative monitoring of alcohol precipitation. J Pharm Biomed Anal 77: 32–39.

Khooshechin S, Safdari J, Moosavian MA, Mallah MH (2013) Prediction of pressure drop in liquid–liquid pulsed packed extraction countercurrent columns. Int J Heat Fluid Flow 44: 684–691.

Kuligowski J, Carrión D, Quintás G, Garrigues S, de la Guardia M (2012) Direct determination of polymerised triacylglycerides in deep-frying vegetable oil by near infrared spectroscopy using Partial Least Squares regression. Food Chem 131: 353–359.

Li J, Jiang Y, Fan Q, Chen Y, Wu R (2014) Simultaneous determination of the impurity and radial tensile strength of reduced glutathione tablets by a high selective NIR-PLS method. Spectrochimica Acta Part A: Mol Biomol Spectroscopy 125: 278–284.

Li W, Cheng Z, Wang Y, Qu H (2013) Quality control of Lonicerae Japonicae Flos using near infrared spectroscopy and chemometrics. J Pharm Biomed Anal 72: 33–39.

Liu H, Chen YF, Li F, Zhang HY (2013) Fructus Gardenia (Gardenia jasminoides J. Ellis) phytochemistry, pharmacology of cardiovascular, and safety with the perspective of new drugs development. J Asian Nat Prod Res 15: 94–110.

Liu SY, Li WL, Qu HB, Zhao BC, Zhao T (2013) On-line monitoring of extraction process of danhong injection based on near-infrared spectroscopy. Zhongguo Zhong Yao Za Zhi 38: 1657–62.

Luna AS, da Silva AP, Pinho JSA, Ferré J, Boqué R (2013) Rapid characterization of transgenic and non-transgenic soybean oils by chemometric methods using NIR spectroscopy. Spectrochim Acta A: Mol Biomol Spectrosc 100: 115–119.

Namkung H, Lee Y, Chung H (2008) Improving prediction selectivity for on-line near-infrared monitoring of components in etchant solution by spectral range optimization. Anal Chim Acta 606: 50–6.

Ni W, Nørgaard L, Mørup M (2014) Non-linear calibration models for near infrared spectroscopy. Anal Chim Acta 813: 1–14.

Nie P, Xia Z, Sun D-W, He Y (2013) Application of visible and near infrared spectroscopy for rapid analysis of chrysin and galangin in Chinese propolis. Sensors 13: 10539–10549.

Reich G (2005) Near-infrared spectroscopy and imaging: basic principles and pharmaceutical applications. Adv Drug Deliv Rev 57: 1109–43.

Roggo Y, Chalus P, Maurer L, Lema-Martinez C, Edmond A, Jent N (2007) A review of near infrared spectroscopy and chemometrics in pharmaceutical technologies. J Pharm Biomed Anal 44: 683–700.

Schönbichler SA, Bittner LKH, Pallua JD, Popp M, Abel G, Bonn GK, Huck CW (2013) Simultaneous quantification of verbenalin and verbascoside in Verbena officinalis by ATR-IR and NIR spectroscopy. J Pharm Biomed Anal 84: 97–102.

Schaefer C, Lecomte C, Clicq D, Merschaert A, Norrant E, Fotiadu F (2013) On-line near infrared spectroscopy as a Process Analytical Technology (PAT) tool to control an industrial seeded API crystallization. J Pharm Biomed Anal 83: 194–201.

Shi J, Zou X, Huang X, Zhao J, Li Y, Hao L, Zhang J (2013) Rapid detecting total acid content and classifying different types of vinegar based on near infrared spectroscopy and least-squares support vector machine. Food Chem 138: 192–199.

Teye E, Huang X, Dai H, Chen Q (2013) Rapid differentiation of Ghana cocoa beans by FT-NIR spectroscopy coupled with multivariate classification. Spectrochim Acta A: Mol Biomol Spectrosc 114: 183–189.

Wu J, Luo W, Wang X, Cheng Q, Sun C, Li H (2013) A new application of WT-ANN method to control the preparation process of metformin hydrochloride tablets by near infrared spectroscopy compared to PLS. J Pharm Biomed Anal 80: 186–191.

Wu Y, Jin Y, Ding H, Luan L, Chen Y, Liu X (2011) In-line monitoring of extraction process of scutellarein from Erigeron breviscapus (vant.) Hand-Mazz based on qualitative and quantitative uses of near-infrared spectroscopy. Spectrochim Acta A: Mol Biomol Spectrosc 79: 934–939.

Wu Z, Xu B, Du M, Sui C, Shi X, Qiao Y (2012) Validation of a NIR quantification method for the determination of chlorogenic acid in Lonicera japonica solution in ethanol precipitation process. J Pharma Biomed Anal 62: 1–6.

Xiong H, Gong X, Qu H (2012) Monitoring batch-to-batch reproducibility of liquid–liquid extraction process using in-line near-infrared spectroscopy combined with multivariate analysis. J Pharm Biomed Anal 70: 178–187.

Zhang Y, Cong Q, Xie Y, JingxiuYang, Zhao B (2008) Quantitative analysis of routine chemical constituents in tobacco by near-infrared spectroscopy and support vector machine. Spectrochim Acta A: Mol Biomol Spectrosc 71: 1408–1413.

Zhu D, Ji B, Meng C, Shi B, Tu Z, Qing Z (2007) The performance of ν-support vector regression on determination of soluble solids content of apple by acousto-optic tunable filter near-infrared spectroscopy. Anal Chim Acta 598: 227–234.

Zhu D, Ji B, Meng C, Shi B, Tu Z, Qing Z (2008) The application of direct orthogonal signal correction for linear and non-linear multivariate calibration. Chemometrics and Intelligent Laboratory Systems 90: 108–115.